Evaluation of an Ultrahigh Precision X-Ray Optics

Shunji Kitamoto[*,a,b], Norimasa Yamamoto[b], Takayoshi Kohmura[b.c], Kazuharu Suga[a.b] , Hiroyuki Sekiguchi[a,b], Yohei Ohkawa[a], Jun`ichi Kanai[a], Shigeto Chiba[a] ,Jun'ichi Sato[a], Keisuke Sudo[a], and Takeshi Watanabe[a]

[a] Department of Physics, Rikkyo University, 3-34-1, Nishi-Ikebukuro, Toshima-ku Tokyo, 171-8501, Japan;
[b] Research Center of the Advanced Measurement, Rikkyo University, 3-34-1, Nishi-Ikebukuro, Toshima-ku Tokyo, 171-8501, Japan;
[c] Physics Department, Kogakuin University, 2665-1, Nakano-cho, Hachioji, Tokyo, 192-0015, Japan

ABSTRACT

We are developing an ultra high precision soft X-ray telescope. The design of the telescope is a normal incident one for 13.5nm band using Mo/Si multilayers. Two ideas are introduced. One is the optical measurement system in order to monitor the precision of the optics system. The other is the adaptive optics system with a deformable mirror. Using an X-ray-optical separation filter, we can always monitor the deformation of the optics by optical light. With this information, we can control the deformable mirror to compensate the system distortion as a closed loop system.

The telescope system is now integrating and checking by optical light. The shape of the primary mirror is an off-axis paraboloid with a focal length of 2m and an effective diameter of 80mm. This primary mirror was coated by Mo/Si multilayers. The reflectivity of the primary mirror at 13.5nm was ranging from 30 to 50 %. The secondary mirror is a basically flat mirror but actually an deformable mirror with 31 piezo-actuators. The detector is now a wave front sensor (shack-hartmann type). The closed loop control has been performed and factor of 2.4 improvement of the wave front shape has been performed comparing to the un-control case.

Keywords: EUV, X-Ray, Telescope, Adaptive Optics, Multilayers

1. INTRODUCTION

We are developing an ultra high precision X-ray Telescope, named X-ray milli-arc-sec Project (X-mas Project), as a future space mission.

The X-ray Astronomical Satellite "Chandra", launched in 1999, is providing us wonderful X-ray images with an angular resolution of ~0.5 arc-sec and we are enjoying lots of important scientific results [1]. However, the current performance of the image quality of X-rays is still far from the theoretical diffraction limit. The diffraction limit of the telescope is determined by the telescope diameter and the wavelength. If we have a diffraction limit X-ray telescope with ~1 m diameter, the resolution of the order of 1 mas can be achieved.

In order to achieve an X-ray telescope with 1 milli-arc-sec resolution, the requirement of the small-scale roughness of the X-ray optics is roughly several angstrom. This is rather easy. The requirement of the large-scale figure error is

*Correspondence: Email: kitamoto@rikkyo.ne.jp

less than wavelength and is roughly 1nm or less. This value is almost impossible. Since the X-ray telescope must be equipped on a satellite, the thermal distortion and the gravitational distortion make a deformation of more than 10 nm. We are now trying to overcome this difficulty by applying two ideas. One is the monitoring of the optics with optical light. The other is the adaptive optics system. In this paper, we report our current status of this project.

2. TELESCOPE DESIGN

To have large effective area, a normal incident configuration is easier than a grazing incident telescope. For 13.5 nm wave length, Mo/Si multi-layers have more than 70 % reflectivity for the normal incident reflection [2, 3]. Also, the possible precision of the measurement of the shape of the mirror is a few nm. Thus 13.5 nm band is the best choice for the telescope using current technique. Figure 1 is the design of a test telescope. The primary mirror has 80 mm diameter effective area. The shape is an off-axis paraboloid with a 100 mm off from the parabola axis. The focal length is 2000 mm. The optical source, deformable mirror and wave front sensor make it possible to monitor and to correct the shape of the telescope, constructing the adaptive feed-back system. For the X-ray imaging, the X ray-optical separation filter and a back-side CCD will be used.

The performance of some of the components has been described elsewhere [4, 5] and in this paper we describe them briefly.

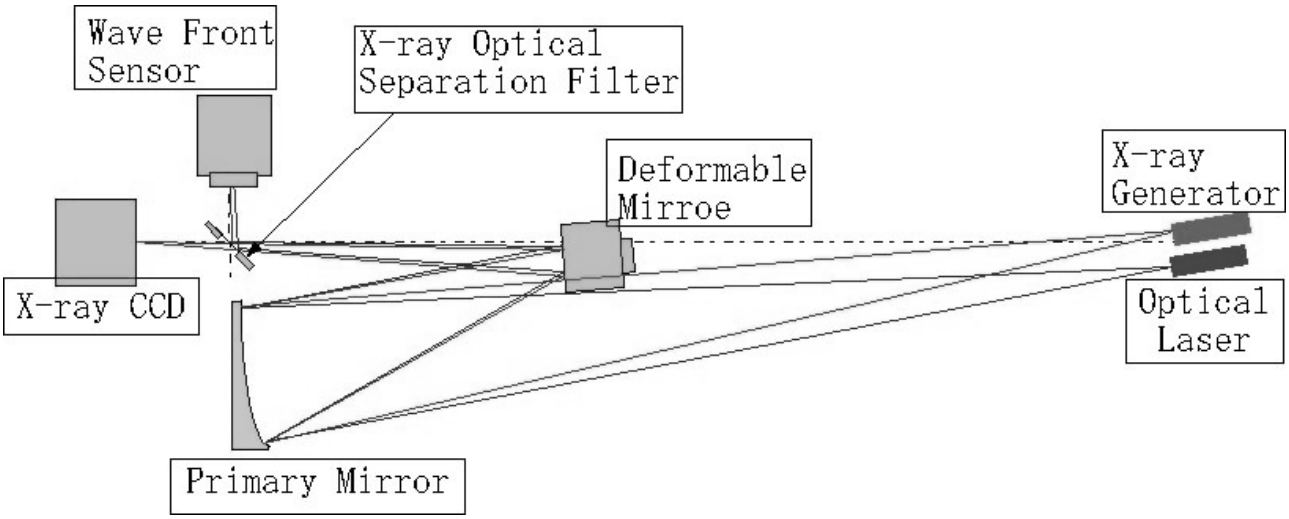

Figure 1. The current design of the laboratory test telescope.

2-1. Wave Front Sensor

The wave front sensor is a shack-hartmann sensor (HASO 31; Imagine Optic) made by a micro-lens array and a CCD [6]. The positions of the images of each micro-lens array are analyzed and the wave front shape is calculated. We have been measured the precision of the image position determination with the CCD and confirmed that the precision is less than 1/100 of the pixel size. The size of the CCD pixel is 10μm, and the position determination accuracy is less than 0.1μm in r.m.s [5].

The ideal spherical waves were exposed to the wave front sensor and checked the measured wave front. The

detected shape of the wave front was ideally spherical within the error of 2nm rms, if the CCD signal was enough high [4].

2-2. X-ray Optical Separation filter

In order to achieve the optical monitoring system, an X ray-optical separation filter is required. In the 13.5nm range, Zr filter has a good transmission [7]. The donuts-shape frame is polished to get a few tenth of nm surface roughness and λ/100 figure error. The 170nm thickness Zr is equipped on the frame. The soft X-ray transmission of this filter was measured with a synchrotron radiation in the Institute of Material Structure Science, High Energy Accelerator Research Organization (KEK-PF). In this beam line, a grazing incident monochrometer is installed with varied-line-spacing plane gratings [8, 9, 10]. By changing the grating, this beam line can provide soft X rays from 80 eV to 1900 eV. Derived X-ray transmission is roughly 50% at 13.5nm range which is corresponding to the transmission of 170 nm thick Zr[4].

2-3. Back side CCD

We have a back-side CCD. The detection efficiency is expected to have roughly 30% for 13.5 nm region. The pixel size is 24 μm. If the angular resolution is 50 mas, the expected image size is 0.5 μm for the 2000 mm focal length. Thus we need finer pixel chip and also we are now developing sub-pixel resolution read-out method [11]. One X-ray event makes an island of spreading charges over several pixels. Thus the center of the image makes the position resolution better than the pixel size. Especially in the case of the bask side CCD, low energy X-rays are absorbed near the exposed plane. Since the electrons must drift to the electrodes, the diffusion makes the electron to spread. The standard deviation of the images, required to calculate the center of the signal, is roughly 0.3 pixels. The 13.5 nm X-rays makes roughly 25 electron-hale pairs. Thus the position determination accuracy is roughly 1/5 of the standard deviation. If we use the CCD with 25 μm pixels, this value is still factor of three larger than expected image size. The required pixel size is less than 10 μm[5].

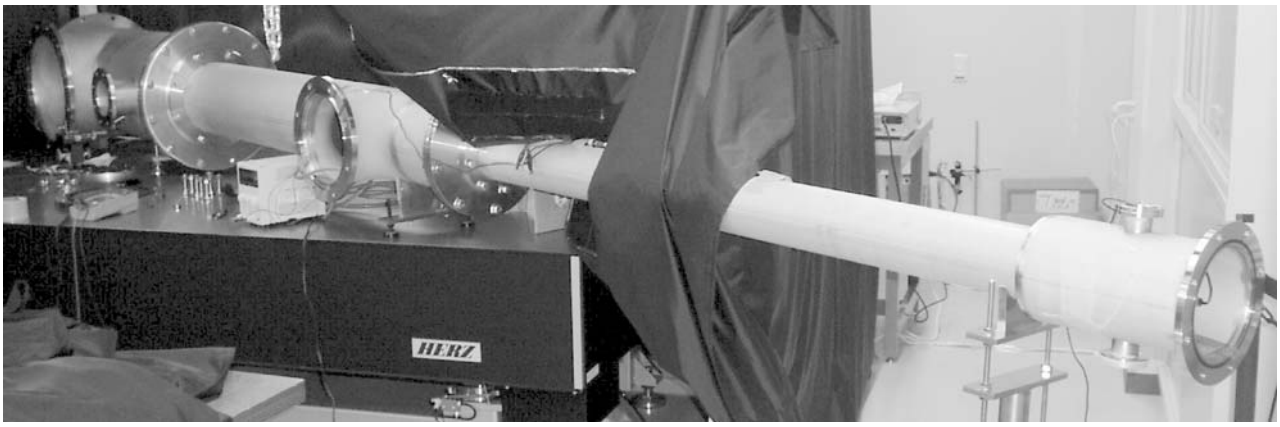

Figure 2. The picture of the vacuum chamber as a telescope. The telescope is on a vibration isolation table.

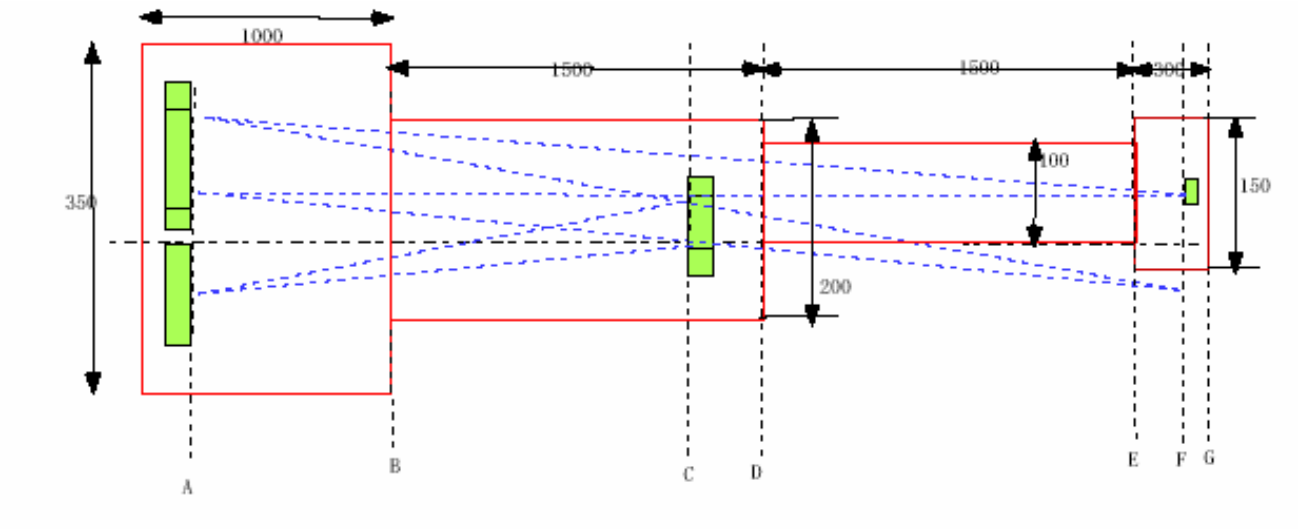

Figure 3. Schematic illustration of the vacuum chamber. The scale of the vertical direction and the horizontal direction is different. The light source is at the right side and the primary mirror is installed at the upper left side. The deformable mirror as a secondary mirror is at the center and the final wave front was measured by the wave front sensor at the lower left.

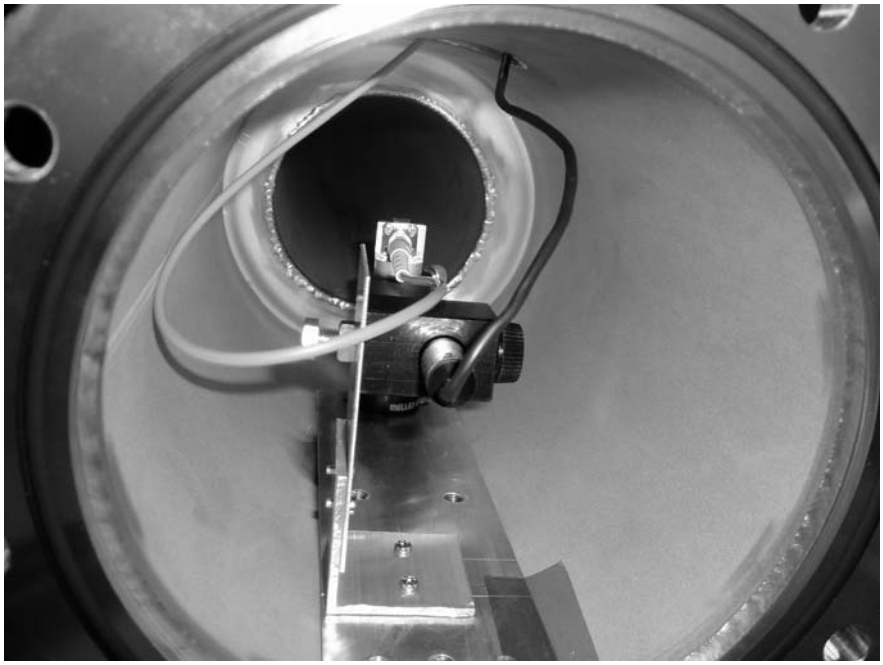

Figure4. The pin-hale laser source and the alignment laser sources. The pin hole source is behind the alignment laser source.

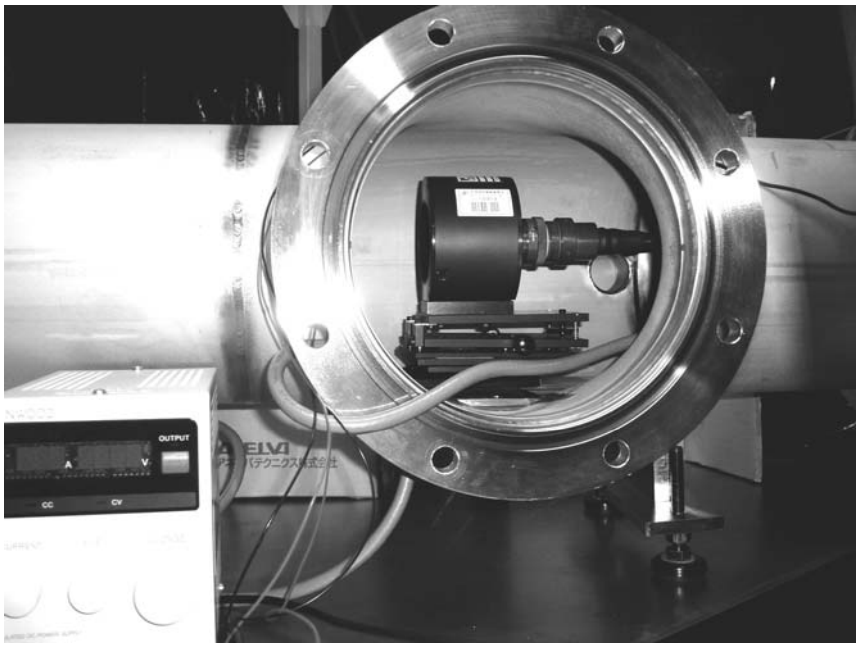

Figure 5. The deformable mirror as the secondary mirror.

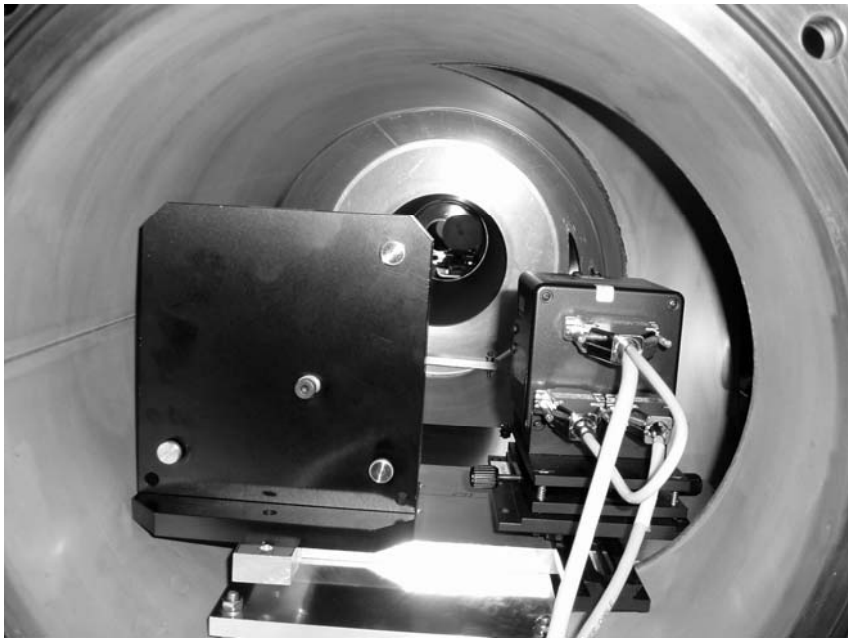

Figure 6. The primary mirror (left) and the wave front sensor (right).

3. TELESCOPE ASSEMBRY

3.1 .Vacuum chamber

All the telescope components must be installed in a vacuum chamber. The picture of the current set up is shown in figure 2. The schematic illustration is shown in figure 3. The vacuum chamber is constructed by three parts according to the required diameter. Now, we are investigating the closed loop performance with the primary mirror and the deformable secondary mirror. Thus only optical light is used and the experiment has been done in the atmospheric condition.

The each component in the vacuum chamber is shown in figure 4, 5, and 6. The vacuum chamber is now on a vibration isolation table.

3.2. Optical light source and alignment laser

Figure 4 shows the picture of the optical light source. The optical light from a laser diode is introduced to an optical fiber. The light is extracted through a $1\mu\mathrm{m}$ pin-hole and the ideal spherical wave is generated, A normal laser source is also equipped near the pin-hole laser source, for the alignment of the optical system.

3.3. Deformable mirror

The deformable mirror is constructed by 31 element bimorph piezo-electric plates (BIM31 mad by CILAS) [12]. One element is at the center, and six elements make a circle around the center and on the seconds and 3rd circle 12 elements are distributed. The elements in the 3rd circle are out of the effective area and they will make the boundary shape of the effective area. The bimorph piezo-electic plate is a two-layer-piezos with the opposite polarity. Thus this plate makes a curvature of concave or convex shape. The effective diameter is 55 mm.

The performance as a single component of the deformable mirror is demonstrated by making a flat plane. Currently 5.26nm-rms of the flatness has been achieved using the feedback system with the Zygo interferometer, although this was done by the different system.

The spherical wave from the light source with a pin hole was first reflected by a paraboroid primary mirror with the diameter of 80mm. The deformable mirror is basically a flat secondary mirror. Monitoring the wave front shape around the focal plane, this deformable mirror is controlled to make a best image.

3.4. Primary Mirror

The left side of the figure 6 shows a picture of the primary mirror. The primary mirror is made by Elide polishing [13]. Its shape is an off-axis paraboloid with an effective diameter of 80 mm and focal length of 2000 mm. Mo/Si multi-layers were coated on the mirror surface and the reflectivity has been measured at 13 positions. The reflectivity is a little worth, but is ranging from 30% to 50%. The diffraction limit of the image size of 80mm diameter for the 13.5nm wave length is ~50 milli-arc-sec.

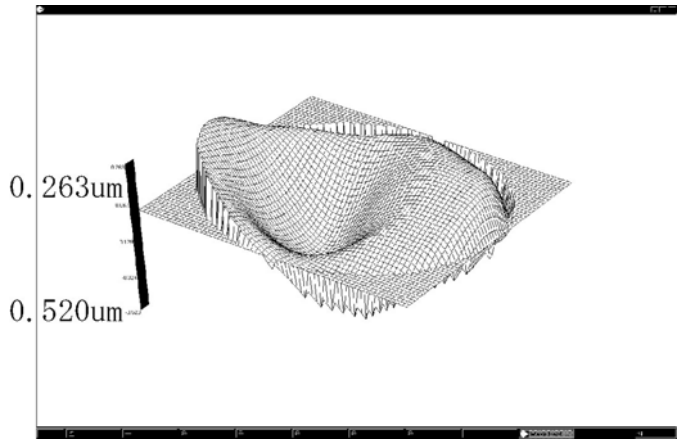

Figure 7. The wave front shape with no control after removing the tilt and focus components.

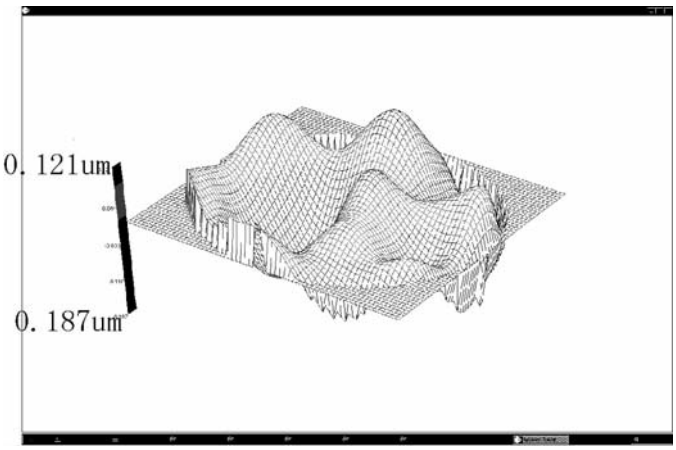

Figure 8. The wave front shape with closed loop control.

4. WAVE FRONT MEASUREMENT

The wave front was measured with the configuration shown in figure 2 and 3. First, the wave front was measured with the reset shape of the deformable mirror (all biases are 0 V). Now the alignment is rough and large tilt and de-focus component is remaining. The PV variation of the wave front is 18.6 μm, and rms variation is 4.69μm. After remove the tilt and de-focus component, the PV and rms variation is 0.783 and 0.143 μm, respectively. The measured wave front shape after removing the tilt and de-focus component is shown in figure 7. Then the closed loop control was started to achieve the wave front to show the spherical shape with the measured tilt component. The PV and rms variation of residual deformation is 0.307 and 0.060 μm. Although this value is much worth than expected,

the correct function of the closed loop has been confirmed. Even in this bad condition, we confirmed the factor of 2.4 improvement of the wave front shape.

5. CONCLUSION

Now we are preparing the vacuum test of the normal incident X-ray telescope with the closed loop system. For the first step, the optical testing in the chamber has been conducted and the appropriate function of the close loop system is confirmed. The other parts for the X-ray testing are still preparing. The X-ray optical separation filter is now scheduling to install the telescope system. The connection of the telescope and the X-ray generator is now designing. The X-ray detector is now a back side CCD. This pixel size is not enough small, but the function test using X-ray can be performed.

6. ACKNOWLEDGMENTS

The author (S.K.) gratefully acknowledges the financial support of the Grant-in-Aid for Scientific Research (Grant No. 14654039 and No. 15037208) .The author (N.Y.) is also supported by the Grant-in-Aid for Scientific Research (Grant No. 16540221). This study is carried out as a part of “Ground-based Research Announcement for Space Utilization” promoted by Japan Space Forum.

REFERENCES

1. Home Page of Chandra X-ray Observatory Center, http://chandra.harvard.edu/
2. E. Luis, A.E. Yakshin, P.C. Gorts, S. Adbali, E.L.G. Maas, R. Stuik and F. Bijkerk 1999, SPIE, 3676, 844-845.
3. J.A. Folta, S. Bajt, W. Barbee, R.F.Grabner, P.B.Mirkarimi, T. Nguyen, M.A. Schmidt, E. Spiller, C.C. Walton, M.Wedowski and C.Montcalm, 1999, SPIE, 3676, 702-809.
4.S. Kitamoto et al. 2003, SPIE 5037, p294.
5. S. Kitamoto et al. 2003, SPIE 5169, p268
6. HASO manual, Imagin Optic
7. B. L. Henke, E. M. Gullikson and J.C. Davis, Atomic Data and Nuclear Data Tables, 54, 181-342 (1993).
8. K. Amemiya, Y. Kitajima, T. Ohta and K. Ito, J. Synchrotron Radiat. 3, 282 (1996).
9. K. Amemiya, Y. Kitajima, Y. Yonamoto, T. Ohta, K. Ito, K. Sano, T. Nagano, M. Koeda, H. Sasai, and Y. Harada, Proc. SPIE, 3150, 171 (1997).
10. Y. Kitajima, K. Amemiya, Y. Yonamoto, T. Ohta, T. Kikuchi, T. Kosuge, A. Toyoshima and K. Ito, J. Synchrotron Radiat. 5, 729 (1998).
11. E. Miyata, M. Miki, H. Tsunemi, J. Hiraga, H. Kouno, K. Miyaguchi, JJAP Express Letter, 2002, 41 L500-501
12. BIM31 Deformable Mirror Assembly User’s Manual, CILAS
13. H. Ohmori, S. Moriyasu, W. Li, and I. Takahashi 1999, Materials and Manufacturing Processes , 14, 1-12,